Poggio, T. & Edelman, S. A network that learns to recognize 3D objects. Nature 343, 263–266

Article *in* Nature · February 1990

DOI: 10.1038/343263a0 · Source: PubMed

TABLE 2 Probability of fecundity in macaques

	Male reared	Female reared
Mother's rank		
Dominant	0.80 (5)	0.92 (14)
Subordinate	0.62 (8)	0.00 (4)

Probability of subordinate and dominant macaques giving birth the year after rearing sons versus daughters. Number of births sampled are given in parentheses. The generalized linear model for macaques only incorporated the variables dominance, sex, and dominance–sex interaction (see Table 1).

quite different in ungulates and primates. In red deer, goats, and bison, as well as in African elephants[9,14,15], sons are suckled more frequently than are daughters during the peak period of lactation and the energetic costs of rearing males probably exceed those of rearing females[9]. Subordinate females could be more strongly affected by these differences because they do not have priority of access to the best feeding sites, and because their body condition is generally poorer than that of dominant females[10]. By contrast, no overall differences in suckling were found between male and female infants in rhesus macaques. But, when the interaction between infant sex and maternal rank was examined, it was found that daughters of subordinate mothers tended to be suckled more frequently than their sons, and more than the infants of dominant mothers[5]. Allowing frequent access to the nipple could have been a maternal response to the high levels of aggression and harassment that the daughters of subordinate mothers tended to receive from unrelated females, a phenomenon which has been documented in several studies[7,16]. Frequent nipple stimulation inhibits ovulation in mammals[17], and this could have been responsible for the longer delays before the next conception among subordinate females that had reared daughters[5,18].

Consequently, the results presented here indicate that two separate selection pressures can favour the evolution of the contrasting sex-ratios in ungulates[1,19–21] and cercopithecine primates[3–7]. First, maternal rank can have opposite effects on the relative fitness of sons and daughters[1,2,6,7]. Second, maternal rank can modify the relative costs of rearing sons and daughters, favouring the production of daughters by subordinate mothers in red deer, and the production of sons by subordinate mothers in macaques. In both cases, these biases could favour the production of an excess of the other sex by dominant females[22]. □

Received 20 July; accepted 27 November 1989.

1. Clutton-Brock, T. H., Albon, S. D. & Guinness, F. E. *Nature* **308,** 358–360 (1984).
2. Clutton-Brock, T. H., Albon, S. D. & Guinness, F. E. *Anim. Behav.* **34,** 460–461 (1986).
3. Simpson, M. J. A., Simpson, A. E., Hooley, J. & Zunz, M. *Nature* **290,** 49–51 (1981).
4. Simpson, M. J. A. & Simpson, A. E. *Nature* **300,** 440–441 (1982).
5. Gomendio, M. thesis, Univ. Cambridge (1988).
6. Altmann, J. *Baboon Mothers and Infants* (Harvard University Press, 1980).
7. Silk, J. B. *Am. Nat.* **121,** 56–66 (1983).
8. Ritchie, M. *Am. Nat.* (in the press).
9. Clutton-Brock, T. H., Albon, S. D. & Guinness, F. E. *Nature* **289,** 487–489 (1981).
10. Clutton-Brock, T. H., Guinness, F. E. & Albon, S. D. *Red Deer: Behaviour and Ecology of Two Sexes* (University of Chicago Press, 1982).
11. Clutton-Brock, T. H., Albon, S. D. & Guinness, F. E. *Nature* **337,** 260–262 (1989).
12. McCullough, P. & Nelder, J. A. *Generalized Linear Models* (Chapman & Hall, London, 1983).
13. Cox, D. R. *The Analysis of Binary Data* (Methuen, London, 1970).
14. Pickering, S. P. C. thesis, Univ. Durham (1983).
15. Lee, P. C. and Moss, C. J. *Behavl Ecol. Sociobiol.* **18,** 353–361 (1986).
16. Dittus, W. P. J. *Behaviour* **69,** 265–302 (1979).
17. McNeilly, A. S. in *The Physiology of Reproduction* (eds Knobil, E. & Neill, J.) 2323–2349 (Raven, New York, 1988).
18. Gomendio, M. *J. Zool.* **217,** 449–467 (1989).
19. Wolff, J. O. *Behavl Ecol. Sociobiol.* **23,** 127–133 (1988).
20. Dhillon, J. S., Acharya, R. M., Tiwana, M. S. & Aggarwal, S. C. *Anim. Prod.* **12,** 81–87 (1970).
21. Singh, O. N., Singh, R. N. & Srivastava, R. R. P. *Ind. J. vet. Sci.* **35,** 245–248 (1965).
22. Fisher, R. A. *The Genetical Theory of Natural Selection* (Oxford University Press, 1930).

ACKNOWLEDGEMENTS. We thank Robert Hinde and Pat Bateson for providing facilities at Madingley, the MRC for access to the macaque colony, the director of the Nature Conservancy Council (Scotland) and the staff of the NCC for permission to work on Rhum, and all those who have helped on the Rhum red deer project for assistance with collecting data on reproductive success and survival. The research was funded by NERC, SERC, the Royal Society, St John's College and Trinity Hall.

A network that learns to recognize three-dimensional objects

T. Poggio & S. Edelman

Artificial Intelligence Laboratory, Center for Biological Information Processing, Massachusetts Institute of Technology, Cambridge, Massachusetts 02139, USA

THE visual recognition of three-dimensional (3-D) objects on the basis of their shape poses at least two difficult problems. First, there is the problem of variable illumination, which can be addressed by working with relatively stable features such as intensity edges rather than the raw intensity images[1,2]. Second, there is the problem of the initially unknown pose of the object relative to the viewer. In one approach to this problem, a hypothesis is first made about the viewpoint, then the appearance of a model object from such a viewpoint is computed and compared with the actual image[3–7]. Such recognition schemes generally employ 3-D models of objects, but the automatic learning of 3-D models is itself a difficult problem[8,9]. To address this problem in computational vision, we have developed a scheme, based on the theory of approximation of multivariate functions, that learns from a small set of perspective views a function mapping any viewpoint to a standard view. A network equivalent to this scheme will thus 'recognize' the object on which it was trained from any viewpoint.

Is the need for 3-D range-based or manually specified models real? Structure from motion theorems[10,11], pioneered by Ullman[12], indicate that full information about the 3-D structure of an object represented as a set of feature points (at least five to eight) is present in just two of their perspective views, provided that corresponding points are identified in each view. A view is represented as a $2N$ vector $x_1, y_1, x_2, y_2, \ldots, x_N, y_N$ of the coordinates on the image plane of N labelled and visible feature points on the object. Here, and in most of the following, we assume that all features are visible, as they are in wire-frame objects. The generalization to opaque objects follows by partitioning the viewpoint space for each object into a set of 'aspects'[13], corresponding to stable clusters of visible features. In principle, therefore, having enough 2-D views of an object is equivalent to having its 3-D structure specified.

This line of reasoning, together with properties of perspective projection, indicate (1) that for each object there exists a smooth function mapping any perspective view into a 'standard' view of the object, and (2) that this multivariate function can be synthesized, or at least approximated, from a small number of views of the object. Such a function would be object-specific, with different functions corresponding to different 3-D objects. Furthermore, the application of the function that is specific for one object to the views of a different object is expected to result in a 'wrong' standard view that can be easily detected as such.

Synthesizing an approximation to a function from a small number of sparse data—the views—can be considered as learning an input–output mapping from a set of examples[14,15]. A powerful scheme for the approximation of smooth functions has been recently proposed under the name of Generalized Radial Basis Functions (GRBFs), and shown[14,15] to be equivalent to standard regularization[16,17] and generalized splines (ref. 14; see closely related work by Powell[18], and Broomhead and Lowe[19]). The approximation of $f: R^n \rightarrow R$ is given by

$$f(\mathbf{x}) = \sum_{\alpha=1}^{K} c_\alpha G(\|\mathbf{x} - \mathbf{t}_\alpha\|) \quad (1)$$

where the K coefficients c_α and the centres $\mathbf{t}_\alpha$ are found during the learning stage and G is an appropriate basis function (see refs 14 and 15), such as the gaussian function. A polynomial term of the form $\sum_i d_i p_i(\mathbf{x})$ can be added to the right-hand side of equation (1). In this paper we omit the polynomial term (see

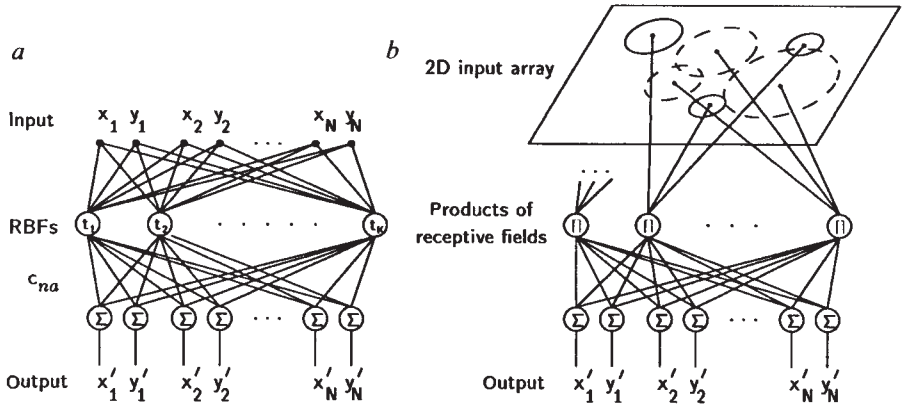

FIG. 1 *a*, Network representation of approximation by GRBFs. In a special simple case, there are as many basis functions (K) as views in the training set (M; in general, $K \leq M$). The centres of the radial functions are then fixed and are identical with the training views. Each basis unit in the 'hidden' layer computes the distance of the new view from its centre and applies to it the radial function. The resulting value $G(\|\mathbf{x}-\mathbf{t}_\alpha\|)$ can be regarded as the 'activity' of the unit. If the function G is gaussian, a basis unit will attain maximum activity when the input exactly matches its centre. The output of the network is the linear superposition of the activities of all the basis units in the network. *b*, An equivalent interpretation of *a* for the case of gaussian radial basis functions. A multidimensional gaussian function can be synthesized as the product of 2-D gaussian receptive fields operating on retinotopic maps of features. The solid circles in the image plane represent the 2-D gaussian functions associated with the first radial basis function, which corresponds to the first view of the object. The dotted circles represent the 2-D receptive fields that synthesize the gaussian radial function associated with another view. The gaussian receptive fields transduce positions of features represented implicitly as activity in a retinotopic array, and their product 'computes' the radial function without the need of calculating norms and exponentials explicitly.

ref. 14). If the function f is vector-valued, each component f_i is computed using equation (1) with the appropriate $c_{i\alpha}$, in which case the equation is equivalent to the network of Fig. 1.

The weights c are found during learning by minimizing a measure of the error between the network's prediction and the desired output for each of the M examples. Computationally, this amounts to inverting a matrix (when $M \neq K$, the generalized inverse is computed instead). When the number of basis functions is less than the number of views in the training set, the centres of the basis functions are also updated during learning. Updating the centres is equivalent to modifying the corresponding 'prototypical views'. For a detailed description of this approximation technique, of its theoretical motivation and its relation to other techniques such as backpropagation[20], see refs 14 and 15.

Figure 2 shows an application of GRBFs to the recognition problem. We consider here the special case of recognizing a wire-frame 3-D object from any of its perspective views with N feature points (we mainly used $N = 6$). A GRBF module, trained on several tens of random views, maps any new view of the same object into a standard view (for example, into one of the initially chosen training views).

We have also explored the use of fewer basis functions than training views and used gradient descent to look for the optimal locations of the centres $\mathbf{t}_\alpha$ in addition to the optimal value of c_α. We found satisfactory performance with just two basis units (for 10–40 training views and with the attitude of the object limited to one octant of the viewing sphere). This indicates that a very small number of units are needed for each aspect[13] of an opaque object (compare with ref. 21). It is of interest that after training, the centres of the radial basis units correspond to views that are different from any of the training views.

It should be clear that the scheme proposed here addresses only one part of the problem of shape-based object recognition, the variability of object appearance due to changing viewpoint. The key issue of how to detect and identify image features that are stable for different illuminations and viewpoints is outside the scope of this paper. Notice that the GRBF approach to recognition does not require the x, y coordinates of image features as inputs: other parameters of appropriate features could also be used, such as a corner angles (see Fig. 4*a*) or segment lengths (compare ref. 4 and M. Villalba, thesis in preparation), or the colour and the texture of the object. Recognition of noisy and partially occluded objects, using realistic feature identification schemes, requires an extension of the scheme, even if the problems of object segmentation and selection[22] are addressed separately. A natural extension of the scheme could be based, for example, on the use of multiple lower-dimensional centres, corresponding to different subsets of detected features, instead of one $2N$-dimensional centre for each view in the example set. Our initial experiments[23] support the notion that a scheme based on low-dimensional centres is useful for recognition while being robust against occlusions and noise. Another possible extension of the scheme involves a hierarchical composition of GRBF modules, in which the outputs of lower-level modules assigned to detect objects parts and their relative disposition in space are combined to allow recognition of complex-structured objects.

In a sense, the application of the GRBF method to recognition can be considered as a generalization of the exact approach of Basri and Ullman[24]. They have recently shown that under orthographic projection, any view of a 3-D object undergoing a linear group of transformations that includes rigid transformation in 3-D space (that is, translations and rotations) can be obtained from three fixed views. They used this result to synthesize a linear operator that, for orthographic projection, maps exactly

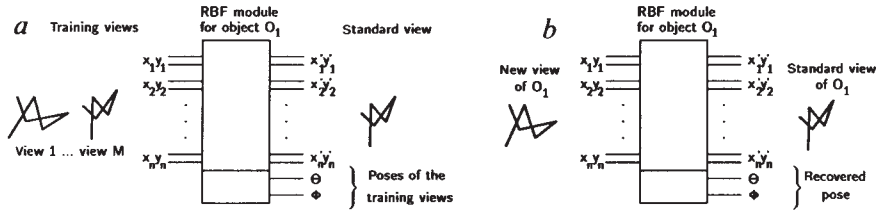

FIG. 2 Application of a general module for multivariate function approximation to the problem of recognizing a 3-D object from any of its perspective views. *a*, Module is trained to produce the vector representing the standard view of the object, given a set of examples of random perspective views of the same object. The module is also capable of recovering the viewpoint coordinates θ, ϕ (the latitude and the longitude of the camera on an imaginary sphere centred at the object) that correspond to the training views. When given a new random view of the same object (*b*), the module recognizes it by producing the standard view. Other objects are rejected by thresholding the euclidean distance between the actual output of the model and the standard view (this step corresponds to the action of a single radial function with a sharp cut-off centred on the standard view).

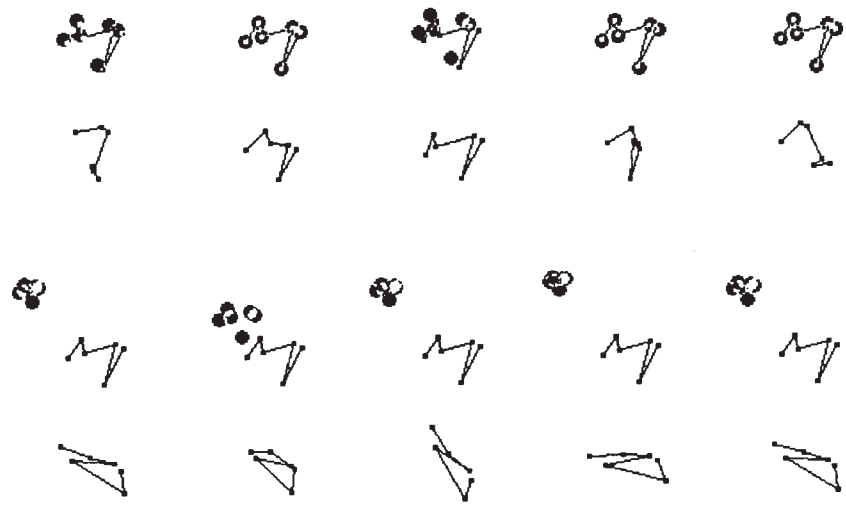

FIG. 3 Some examples of the module's operation. Standard view of a wire-frame object (top row) superimposed on its estimate by the GRBF network (large dots) when its input is a random view of the same object (second row from top). The fit is much closer than in the bottom two rows, where the input view belongs to a different object. The number of training views M is 40, the number of RBFs K is 20, and the range of attitudes θ, ϕ is 0°–90°. Gradient descent was used to obtain the optimal positions of the GRBF centres. Within a smaller range of θ, $\phi \in [0°, 45°]$, the performance was acceptable with only two radial basis units ($M=40$, $K=2$).

each view of a given object into the zero vector and performs fairly well also for most cases of perspective projection[24]. By comparison, the GRBF approach is based on an approximation, even in the orthographic case, and typically needs more than three views. But it can (1) use as inputs feature parameters other than the x, y coordinates (Fig. 4a) and (2) recover parameters, such as the attitude angles of the input object (Fig. 4d), that do not depend linearly on the views of the object.

In some respects, the performance of the GRBF-based recognition scheme resembles human performance in a related task. For example, the number of training views necessary to achieve an acceptable recognition rate on novel views, 80–100 for the full viewing sphere, is broadly compatible with the finding[25] that people have trouble recognizing a novel wire-frame object previously seen from one viewpoint if it is rotated away from that viewpoint by about 30° (it takes 72 30°×30°-patches to cover the viewing sphere). Furthermore, a network model recently shown to capture some of the time-course and learning characteristics of the recognition process[26], seems to be computationally related to GRBFs[27]. Experiments designed to test specific predictions of GRBF and several other recognition schemes[24,27] are now under way in our laboratory.

One feature of the GRBF scheme that could guide its interpretation in biological terms is the possibility of decomposing a multidimensional gaussian radial basis function into a product of gaussian functions of lower dimensions (Fig. 1b). In our case, the centre of a basis unit is similar to a prototype and the unit itself is synthesized as the product of feature detectors with 2-D gaussian receptive fields (that is, the activity of a detector depends on the distance r between the stimulus and the centre of the receptive field as e^{-r^2/σ^2}). The network's output (see equation 1) is the sum of products and therefore represents the logical disjunction of conjunctions '$\vee_\alpha \wedge_i$ (feature F_i at (x_i, y_i))', where the disjunction ranges over all the protypes of the given object.

The adjustment of weights c_α in the GRBF network in Fig. 1 through some pseudo-hebbian mechanism is not biologically implausible. Alternatively, a plausible biophysical implementation of the gradient-descent update of the centres (or, as in Fig. 1b, the location of the receptive fields) is problematic. But notice that reasonable initial performance can be obtained merely by setting the centres to a subset of the examples. A subsequent possibly slow process, much simpler and more plausible than gradient descent, may then search for optimal positions. Another possible solution is to select for each object a set of optimally located receptive fields out of a large available population[27,14].

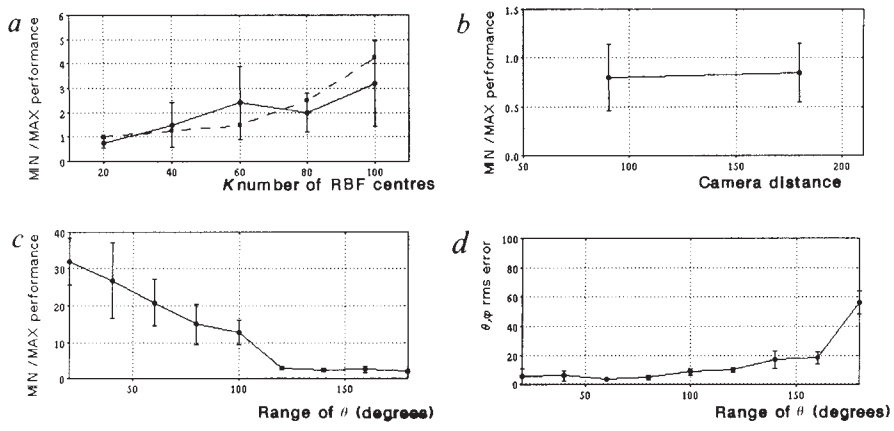

FIG. 4 a, Performance of a GRBF module trained to recognize a specific object over the full range of θ, ϕ (the entire viewing sphere). Views were encoded as vectors of $2N$ vertex coordinates (solid curve; error bars show the s.d. of the performance indices, computed over a set of 10 objects, each of which served in turn as the target) or as vectors of $N-2$ angles formed by pairs of segments (dashed curve). In these examples, the number of training views M is chosen to equal the number of radial basis functions K. The performance index MIN/MAX is defined as the ratio of the smallest euclidean distance E obtained for views of different objects to the largest E obtained over a set of novel random views of the object on which the module has been trained. MIN/MAX > 1 is required for a perfect separation between the target and other objects using a simple threshold decision. For nearly perfect recognition, 80–100 views suffice. b, Performance for two conditions—near and far—corresponding to relatively high and low perspective distortion, respectively (full range of θ, ϕ in both cases). c, GRBF shows a slow degradation in performance with increasing range of the viewpoint coordinates θ, ϕ (the objects are a cube and an octahedron, $M=K=40$, and the error bars are s.d. over 10 sets of random training and testing views). d, GRBF can also provide a good estimate of the attitude of the object. The inset shows the errors in the viewpoint coordinates θ, ϕ recovered by the module versus the range of the viewpoint coordinates. In c and d, $\phi_{max}=2\theta_{max}$, so that $\theta_{max}=180°$ corresponds to the full viewing sphere.

Sensory-input driven selection of representation units has been demonstrated *in vivo* (for example, see refs 28 and 29).

The GRBF recognition scheme seems reasonable in terms of the biophysical mechanisms required, is attractive because an effective computation is simply performed by the combination of receptive fields, and is surprising because it bases a scheme involving units somewhat similar to 'grandmother' cells (compare refs 30 and 31) on the rigorous approximation methods of regularization and splines. □

Received 9 August; accepted 20 November 1989.

1. Marr, D. *Vision* (Freeman, San Francisco, 1982).
2. Poggio, T., Gamble, E. B. & Little, J. J. *Science* **242,** 436–440 (1988).
3. Fischler, M. A. & Bolles, R. C. *Commun. ACM* **24,** 381–395 (1981).
4. Thompson, D. W. & Munday, J. L. in *Proc. IEEE Conf. Robotics and Automation* 208–220 (Raleigh, North Carolina, 1987).
5. Huttenlocher, D. P. & Ullman, S. in *Proc. 1st Int. COnf. Computer Vision* 102–111 (IEEE, Washington DC, 1987).
6. Lowe, D. G. *Perceptual Organization and Visual Recognition* (Kluwer Academic Publishers, Boston, Massuchusetts, 1986).
7. Ullman, S. *Cognition* **32,** 193–254 (1989).
8. Grimson, W. E. L. & Lozano-Pérez, T. *IEEE Trans. Pattern Analysis Machine Intell.* **9,** 469–482 (1987).
9. Fan, T. J., Medioni, G. & Nevatia, R. in *Proc. 2nd Int. Conf. Computer Vision* 474–481 (Florida, IEEE, Washington DC, 1988).
10. Tsai R. Y. & Huang, T. S. *IEEE Trans. Pattern Analysis Machine Intell.* **6,** 13–27 (1984).
11. Longuet-Higgins, H. C. *Nature* **293,** 133–135 (1981).
12. Ullman, S. *The Interpretation of Visual Motion* (MIT Press, Cambridge, Massachusetts, 1979).
13. Koenderink, J. J. & van Doorn, A. J. *Biol. Cybern.* **32,** 211–217 (1979).
14. Poggio, T. & Girosi, F. *Artif. Intell. Lab. Memo No. 1,140* (Artificial Intelligence Laboratory, MIT, Cambridge, 1989).
15. Poggio, T. & Girosi, F. *Science* (in the press).
16. Tikhonov, A. N. & Arsenin, V. Y. *Solutions of Ill-posed Problems* (Winston, Washington DC, 1977).
17. Poggio, T., Torre, V. & Koch, C. *Nature* **317,** 314–319 (1985).
18. Powell, M. J. D. in *Algorithms for Approximation.* (eds Mason, J. C. & Cox, M. G.) (Clarendon, Oxford, 1987).
19. Broomhead, D. S. & Lowe, D. *Complex Syst.* **2,** 321–355 (1988).
20. Rumelhart, D. E., Hinton, G. E. & Williams, R. J. *Nature* **323,** 533–536 (1986).
21. Perrett, D. I., Mistlin, A. J. & Chitty, A. J. *Trends Neurosci.* **10,** 358–364 (1989).
22. Edelman, S. & Poggio, T. *Optic News* **15,** 8–15, May 1989.
23. Poggio, T. & Edelman, S. *Artif. Intell. Lab. Memo No. 1,181* (Artificial Intelligence Laboratory, MIT, Cambridge, 1989).
24. Basri, R. & Ullman, S. *Artif. Intell. Lab. Memo No. 1,152* (Artificial Intelligence Laboratory, MIT, Cambridge, 1989).
25. Rock, I. & DiVita, J. *Cognitive Psychol.* **19,** 280–293 (1987).
26. Edelman, S., Bülthoff, H. & Weinshall, D. *Artif. Intell. Lab. Memo No. 1,138* (Artificial Intelligence Laboratory, MIT, Cambridge, 1989).
27. Edelman, S. & Weinshall, D. *Artif. Intell. Lab. Memo No. 1,146* (Artificial Intelligence Laboratory, MIT, Cambridge, 1989).
28. Jenkins, W. M., Merzenich, M. M. & Ochs, M. T. *Soc. Neurosci. Abstr.* **10,** 665 (1984).
29. Edelman, G. M. & Finkel, L. in *Dynamical Aspects of Neocortical Function* (eds Edelman, G. M., Gall, W. E. & Cowan, W. M.) 653–695 (Wiley, New York, 1984).
30. Gross, C. G., Rocha-Miranda, C. E. & Bender, D. B. *J. Neurophys.* **35,** 96–111 (1972).
31. Perrett, D. I., Rolls, E. T. & Caan, W. *Expl Brain Res.* **47,** 329–342 (1982).

ACKNOWLEDGEMENTS. We thank F. Crick, F. Girosi, E. Grimson, E. Hildreth, D. Hillis, A. Hurlbert, L. Tucker, S. Ullman and D. Weinshall for discussion. The work was done in the Artificial Intelligence Laboratory and the Center for Biological Information Processing in the Department of Brain and Cognitive Sciences. This research was supported by the ONR, Cognitive and Neural Sciences Division, and the Artificial Intelligence Center of Hughes Aircraft Corporation. Support for the A.I. Laboratory's artificial intelligence research is provided by the Advanced Research Projects Agency of the Department of Defense. T.P. is supported by the Uncas and Helen Whitaker chair. S.E. is supported by a Chaim Weizmann Postdoctoral Fellowship from the Weizmann Institute of Science.

A second molecular form of D_2 dopamine receptor in rat and bovine caudate nucleus

Christopher L. Chio*, Gerard F. Hess†, R. Scott Graham† & Rita M. Huff*

* Cell Biology and † Molecular Biology, The Upjohn Co., Kalamazoo, Michigan 49001, USA

OVEREXPRESSION of the D_2 dopamine receptor has been proposed to be part of the pathology of schizophrenia[1]. The isolation of a D_2 dopamine receptor clone has assisted the molecular characterization of D_2 receptors[2]. We have now isolated an identical rat clone along with two other clones—a second related rat clone ($RD\text{-}2_{in}$) and a homologous bovine clone ($BD\text{-}2_{in}$), both of which contain an insert encoding an additional 29 amino acids relative to the original rat clone ($RD\text{-}2_o$). All three clones encode D_2 receptor binding sites when expressed in COS-7 cells. The amino-acid insert encoded by $D\text{-}2_{in}$ lies in the domain of the receptor believed to interact with the GTP-binding proteins (G proteins) of various signal transduction pathways[3]. By using oligonucleotide probes specific for either $D\text{-}2_o$ or $D\text{-}2_{in}$ RNA transcripts, we have found that the level of expression of the $D\text{-}2_{in}$-encoded form of the receptor is seven times that of the $D\text{-}2_o$ form in the caudate nucleus, the richest brain source of D_2 receptors[4].

We have isolated a clone, $RD\text{-}2_o$, that was shown by sequencing to be identical (between the *Xho*I and *Pst*I sites) to the rat D_2 clone of Bunzow *et al.*[2] We labelled $RD\text{-}2_o$ complementary DNA with random primer and used it as a hybridization probe to screen a bovine caudate nucleus cDNA library. We identified and isolated a single positive plaque, and found the cloned DNA fragment to comprise 2,376 bases. The DNA sequence and the amino-acid sequence of the longest open reading frame are shown in Fig. 1. Alignment of the bovine clone with $RD\text{-}2_o$ showed that the two clones are highly homologous, except that the bovine clone contains an insert of 87 nucleotides that is not found in $RD\text{-}2_o$. Thus, the bovine clone encodes a protein of 444 amino acids compared with the 415 amino acids encoded by $RD\text{-}2_o$. Excluding the insert, the clones from the two species are 85% identical at the nucleotide sequence level and 96% identical at the amino-acid sequence level, with the few amino-acid differences being conservative changes.

Further screening of the original rat brain cDNA library revealed that of 16 positive clones, 4 had cloned DNA fragments of ~1,450 bases (one of these is $RD\text{-}2_o$), and 12 had cloned DNA fragments of ~1,550 bases. DNA from a clone of ~1,550 bases, clone $RD\text{-}2_{in}$, was sequenced and found to be identical to $RD\text{-}2_o$, including the noncoding sequence between the *Xho*I and *Pst*I sites, except for an additional 87 nucleotides inserted between nucleotides 723 and 724 of $RD\text{-}2_o$. The additional sequence in $RD\text{-}2_{in}$ is inserted at the same location and is highly similar (97%) to the bovine insert sequence.

D_2 dopamine receptors belong to a family of receptors whose members have in common an interaction with one of the G proteins for signal transduction. All family members sequenced so far have structural similarities, including seven putative transmembrane domains and a putative G protein-coupling domain in the third intracytoplasmic loop[5]. It is in the putative third intracytoplasmic loop of the D_2 dopamine receptor that the additional coding sequences of $RD\text{-}2_{in}$ and $BD\text{-}2_{in}$ are found. The amino-acid sequences encoded by the two rat clones and the bovine clone flanking and including the insert region are shown in alignment in Fig. 2. The amino-acid sequence encoded by the insert in $RD\text{-}2_{in}$ is identical to that encoded by the insert in $BD\text{-}2_{in}$, except for a single methionine-to-valine substitution.

We transfected all three clones into African green monkey kidney cells (COS-7) and measured D_2 binding sites using the D_2 dopamine receptor antagonist [^{3}H]spiroperidol. We detected high and equivalent levels of D_2 receptors in homogenates of COS-7 cells transfected with each clone (Fig. 3). Furthermore, the newly expressed receptors had similarly high affinities for [^{3}H]spiroperidol ($K_d = 18$ pM ($RD\text{-}2_o$); $K_d = 22$ pM ($RD\text{-}2_{in}$); $K_d = 24$ pM ($BD\text{-}2_{in}$); K_d, dissociation constant)—the same as the affinity of the D_2 receptor in the caudate nucleus for spiroperidol and 1,000 times the affinity of the D_1 dopamine receptor for spiroperidol[6]. The affinities of $RD\text{-}2_o$-, $RD\text{-}2_{in}$- and $BD\text{-}2_{in}$-encoded receptors for dopamine in membranes prepared from transfected cells were also nearly identical, at ~1–2 μM.